Journal of Power Sources 244 (2013) 527–531

Contents lists available at SciVerse ScienceDirect

Journal of Power Sources

journal homepage: www.elsevier.com/locate/jpowsour

Short communication

Effects of a dopant on the electrochemical properties of $Li_4Ti_5O_{12}$ as a lithium-ion battery anode material

Jung Soo Park, Seong-Ho Baek, Yong-Il Jeong, Bum-Young Noh, Jae Hyun Kim*

Division of Green Energy Research, Daegu-Gyeongbuk Institute of Science and Technology (DGIST), 50-1, Sang-ri, Hyeonpung-myeon, Dalseong-gun, Daegu 711-873, Republic of Korea

HIGHLIGHTS

- The discharge capacity of LATO was greatly improved with an increasing various composition.
- The discharge capacity of LATO was greatly improved with an increasing calcination temperature.
- Al^{3+} substitution greatly increased both the reversible capacity and cycling stability of $Li_4Ti_5O_{12}$.

ARTICLE INFO

Article history:
Received 13 November 2012
Received in revised form
12 February 2013
Accepted 15 February 2013
Available online 16 March 2013

Keywords:
Lithium-ion batteries
Anode materials
Lithium titanium oxide
Aluminum doping

ABSTRACT

$Li_4Ti_5O_{12}$ and Al^{3+} doped $Li_{(4-x/3)}Al_xTi_{(5-2x/3)}O_{12}$ (x = 0, 0.01, 0.05, 0.1, 0.15, 0.2) are synthesized at 750, 850, 950 °C via solid state reaction using TiO_2-rutile, Li_2CO_3 and Al_2O_3 as precursors. The samples at 850, 950 °C have better phase purity than those at 750 °C. The preliminary charge–discharge cycling test of undoped and Al^{3+} doped $Li_4Ti_5O_{12}$ reveals that the electrochemical performance of the electrode prepared at 850 °C is better than that at 750, 950 °C. Therefore, the optimum calcination temperature is found to be 850 °C. $Li_{(4-x/3)}Al_xTi_{(5-2x/3)}O_{12}$ (x = 0.01, 0.05, 0.1), which is the low Al-doped sample, exhibits a higher discharge capacity and rate performance than the high Al-doped $Li_4Ti_5O_{12}$ (x = 0.15, 0.2) sample. The first discharge capacities at 0.2, 0.5, and 1 C are 174.4, 161.9, and 153.8 mAh g^{-1}, respectively for $Li_{(4-x/3)}Al_xTi_{(5-2x/3)}O_{12}$ (x = 0.1). These values are similar to those of $Li_{(4-x/3)}Al_xTi_{(5-2x/3)}O_{12}$ (x = 0.01, 0.05). The capacity retention ratio of $Li_{(4-x/3)}Al_xTi_{(5-2x/3)}O_{12}$ (x = 0.01, 0.05, 0.1) is over 99.3% after 30 cycles. The capacity increase and good rate performance in the optimum Al-doped $Li_4Ti_5O_{12}$ are discussed in relation to the stability of the spinel structure and the resulting ease of lithium insertion.

1. Introduction

The great success that Li-ion batteries (LIBs) have experienced in portable electronics is being extended to use in electric vehicles. The commercialized LIBs use carbon as the anode material. However, the passivation film is formed during the first charging in the carbonaceous materials, which consumes lithium from the cathode. This passivation layer could decompose at high temperature, inducing failure of the cell and even ignition of the battery [1]. For resolving this safety problem, spinel lithium titanate ($Li_4Ti_5O_{12}$) is a very attractive anode material candidate. It has almost zero volume change during the Li-insertion/extraction process, which leads to a reliable cycle performance. Moreover, it has a flat operating voltage of about 1.5 V, which is higher than the reduction potential of most electrolyte solvents. Therefore, $Li_4Ti_5O_{12}$ has excellent characteristics in regard to the safety issue [2].

The lithium intercalation and deintercalation process of $Li_4Ti_5O_{12}$ have been well characterized [3,4]. The structure of $Li_4Ti_5O_{12}$ belongs to a cubic system with space group Fd3m, 75% of lithium ions occupy tetrahedral 8a sites, and 25% of lithium ions and Ti^{4+} are randomly distributed at octahedral 16d sites. All the oxygen ions are located at the 32e sites. Upon lithium intercalation, the framework remains the same. The incoming lithium ions occupy 16c sites and the lithium ions at 8a sites also shift to 16c sites. Three out of five titanium ions are reduced to Ti^{3+} from Ti^{4+}. When a trivalent metal cation is substituted into $Li_4Ti_5O_{12}$, it is known that the doping metal ions together with the Ti^{4+} occupy the 16d octahedral sites [5,6].

A main obstacle of $Li_4Ti_5O_{12}$ is poor rate capability due to its low electronic conductivity. To overcome this drawback, several approaches have been adopted: doping it with ions [6–19], coating it with a conductive phase [20–24], and using porous structures

* Corresponding author. Tel.: +82 53 785 3610; fax: +82 53 785 3439.
E-mail address: jaehyun@dgist.ac.kr (J.H. Kim).

0378-7753/$ – see front matter © 2013 Elsevier B.V. All rights reserved.
http://dx.doi.org/10.1016/j.jpowsour.2013.02.048

[25,26]. Among the doped samples, the trivalent metal ion doped ones are noteworthy because of their high capacity and good cycling performance. $Li_{(4-x)/3}Ti_{(5-2x)/3}Cr_xO_4$ ($0 \le x \le 0.9$) was prepared by a ceramic technique. The specific capacity increased with an increasing composition of Cr and reached the highest value for the $Li_{1.10}Ti_{1.20}Cr_{0.7}O_4$ compound. It also had the highest capacity values after 50 cycles [5].

Al^{3+} doping in the Ti-site of $Li_4Ti_5O_{12}$ was reported to increase the reversible capacity and cycling stability considerably when the doped $Li_4Ti_5O_{12}$ was charged and discharged [27,28]. The samples in which Al ions were substituted into the Li-site of $Li_4Ti_5O_{12}$ did not have a better rate capability and capacity than undoped $Li_4Ti_5O_{12}$ [29]. The effect of the firing temperature of the sample on the electrochemical performance in a wide range of composition in Al^{3+} doped $Li_4Ti_5O_{12}$ has not been thoroughly investigated until now as far as we know.

The aim of this study was to find the optimum calcination temperature and the composition that had the best electrochemical properties in a wide composition range of Al^{3+} doped $Li_4Ti_5O_{12}$. First, the synthesizing temperature of undoped $Li_4Ti_5O_{12}$ and $Li_{(4-x/3)}Al_xTi_{(5-2x/3)}O_{12}$ ($x = 0.01$) samples varied from 750 °C to 950 °C. After structural and electrochemical characterization of these two compositions, the best calcinations temperature was determined. At the firing temperature, a series of $Li_{(4-x/3)}Al_xTi_{(5-2x/3)}O_{12}$ ($x = 0$, 0.01, 0.05, 0.1, 0.15, 0.2) samples was synthesized and their structural characteristics were investigated by X-ray diffraction and scanning electron microscopy. The rate performance as well as the discharge curves of each sample at different current densities was studied.

2. Experimental

$Li_{4-x/3}Al_xTi_{5-2x/3}O_{12}$ ($x = 0$, 0.01, 0.05, 0.1, 0.15, 0.2) were prepared using a solid state method from stoichiometric mixture of Li_2CO_3 (Aldrich), TiO_2 (Aldrich) and Al_2O_3 (Aldrich). Excessive Li (3 wt.%) was provided to compensate for the loss of Li during synthesis. The precursors were ball-milled for 36 h and dried at 100 °C for 24 h and calcined at 750, 850, 950 °C for 36 h in air. The samples were then cooled to room temperature and ground.

X-ray diffraction (XRD) patterns were collected using an Empyrea X-ray diffractometer with Cu Kα radiation. The morphologies of the electrode materials were investigated with Field Emission Scanning Electron Microscopy (Hitachi, S-4800).

The electrode was prepared from ball-milling of a slurry containing 80 wt.% anode material, 12 wt.% Super P, and 8 wt.% polyvinylidene fluoride (PVDF) dissolved in *n*-methyl pyrrolidone (NMP) solvent. The paste was coated on an aluminum foil by the doctor-blade method. The working electrode was dried at 110 °C in a vacuum oven for 12 h and then pressed into its final thickness of 40–60 μm. After they were completely dried, 14 mm diameter Al sheet electrodes were cut.

Electrochemical cells were assembled in an Ar-filled glove box with metallic lithium foil as the counter electrode, a polypropylene membrane as the separator and 1 M $LiPF_6$ in a mixture of ethyl carbonate (EC) and dimethyl carbonate (DMC) (3:7 vol. ratio) as the electrolyte. The charge/discharge was measured with TOSCAT-3100. The charge/discharge measurement was performed in a potential range of 1.0–3.0 V.

3. Results and discussion

The XRD patterns of the undoped $Li_4Ti_5O_{12}$ and $Li_{(4-x/3)}Al_xTi_{(5-2x/3)}O_{12}$ ($x = 0.01$) that were calcined at 750 °C, 850 °C and 950 °C were analyzed to find the optimum firing temperature. The samples synthesized at 750 °C showed clear impurity peaks due to the TiO_2 second phase. The samples that were fired at 950 °C had XRD peaks similar to the ones at 850 °C in which very few impurity peaks were detected. The XRD patterns of materials at 750 and 950 °C are not shown here. To find the best calcination temperature for optimum electrochemical properties, preliminary cyclic performances were examined for the two $Li_{(4-x/3)}Al_xTi_{(5-2x/3)}O_{12}$ ($x = 0.01$) samples fired at 850 °C and 950 °C. Based on these results, the optimum calcination temperature of this system was found to be 850 °C. A series of Al^{3+} doped $Li_{(4-x/3)}Al_xTi_{(5-2x/3)}O_{12}$ ($x = 0.01$, 0.05, 0.1, 0.15, 0.2) samples synthesized at 850 °C were electrochemically studied.

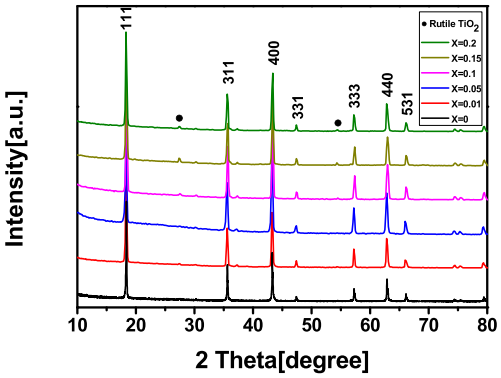

Fig. 1. XRD patterns of $Li_{4-x/3}Al_xTi_{5-2x/3}O_{12}$ ($x = 0$, 0.01, 0.05, 0.1, 0.15, 0.2) synthesized at 850 °C.

The XRD patterns of the Al^{3+} doped $Li_{(4-x/3)}Al_xTi_{(5-2x/3)}O_{12}$ ($x = 0.01$, 0.05, 0.1, 0.15, 0.2) in comparison with the pristine $Li_4Ti_5O_{12}$ are shown in Fig. 1 when the synthesized temperature is 850 °C. All major peaks agreed with the standard diffraction peaks of $Li_4Ti_5O_{12}$. When $x \le 0.1$, the diffraction patterns of all the materials obtained had negligible impurity peaks except for $x = 0.05$ that had no impurity peaks. When x was increased over $x = 0.1$, a TiO_2 phase was clearly detected as evidenced in Fig. 1 for $Li_{(4-x/3)}Al_xTi_{(5-2x/3)}O_{12}$ ($x > 0.1$). The magnified (111) peaks shifted to the lower 2θ angle when the Al^{3+} content was increased to $x = 0.1$ as shown in Fig. 2, which means that the lattice parameter increased with the increasing Al-doping. At $x = 0.15$ and 0.2, the tendency of the lattice parameter increase was not consistent with the one observed in the low Al doped region ($x \le 0.1$). This may be due to impurity segregation, which means that the doped Al ions were not well substituted into the lattice sites of the spinel $Li_4Ti_5O_{12}$ structure. These results are different from previous reports in which it was said that the doped Al ions may substitute only Li-ions [27] or

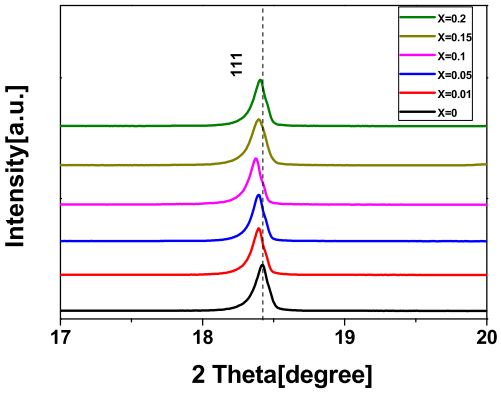

Fig. 2. Enlarged (111) peaks of $Li_{4-x/3}Al_xTi_{5-2x/3}O_{12}$ ($x = 0$, 0.01, 0.05, 0.1, 0.15, 0.2) samples.

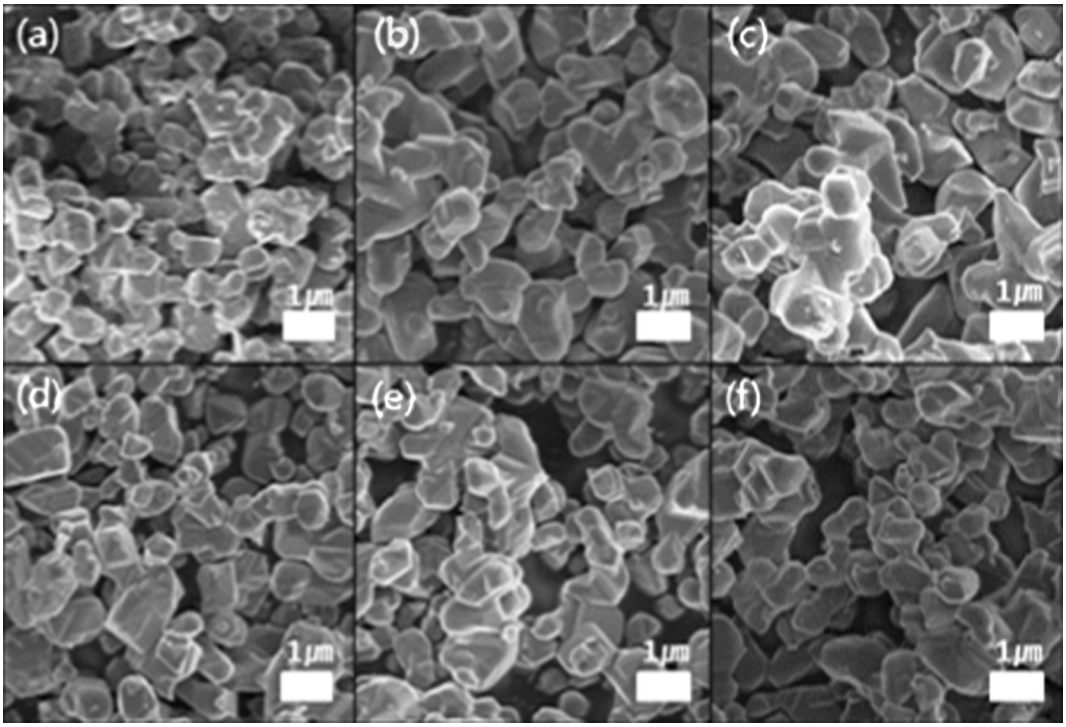

Fig. 3. Typical SEM photographs of $Li_{(4-x/3)}Al_xTi_{(5-2x/3)}O_{12}$ ($0 \le x \le 0.2$) samples prepared at 850 °C, (a) $x = 0$, (b) $x = 0.01$, (c) $x = 0.05$, (d) $x = 0.1$, (e) $x = 0.15$, and (f) $x = 0.2$.

Ti ions [28]. In those cases, the lattice parameter decreased with an increasing Al^{3+} content. Our results might be related to the suggestion that the Al ions occupy both Ti^{4+} and Li^{+} sites [18]. The doped Al ions together with the Ti^{4+} may mainly substitute both Ti^{4+} and Li^{+} of the 16d octahedral sites due to negligible intensity of the (220) peak. The (220) peak is very weak in the normal spinel because these sites are solely occupied by lithium ions at 8a sites [30]. The XRD peak intensities decreased with the doping amount of Al, suggesting the relatively poor crystallinity of Al-doped $Li_4Ti_5O_{12}$.

Typical SEM photographs of $Li_{(4-x/3)}Al_xTi_{(5-2x/3)}O_{12}$ samples prepared at 850 °C are shown in Fig. 3. There is no obvious change in particle size of the pure and Al-doped samples, which is similar to the reports by Huang et al. [28]. All the samples exhibited a particulate shape. The particles had a relative uniform morphology with a narrow size distribution, which was in the range of 0.6–1.2 μm. This may result in sufficient contact between the electrode and electrolyte, facilitating the Li^{+} and electron transportation. The calcination temperature effect on the morphological evolution was also observed. The morphologies of the samples that were synthesized at 750 and 850 °C were similar, but bigger particles were observed in the samples at 950 °C due to grain growth at high temperature (Fig. 4). However, agglomeration to a certain extent between particles was observed in the Al-doped samples.

Fig. 5 shows the anodic capacity as a function of cycle number for $Li_{(4-x/3)}Al_xTi_{(5-2x/3)}O_{12}(x = 0.01)$ at three different calcination temperatures, 750 °C, 850 °C and 950 °C at 1 C. The sample at 850 °C had the highest capacity and best cycling behavior hence that condition was chosen as the optimum process temperature as mentioned in the previous section. The capacity retentions of all three cells were over 99.3% and the values were almost the same. We consider that the electrode prepared at 750 °C had the lowest capacity due to the TiO_2 second phase. The particles at 950 °C were larger than those at 850 °C as shown in Fig. 3. The larger particle size may have resulted in a larger diffusion length for the Li-ions and a lower contact area between the active materials and the electrolyte. Thus, the electrodes calcined at 950 °C exhibited a lower discharge capacity than those at 850 °C, even though the crystallinity of the two samples was very similar in the XRD analysis.

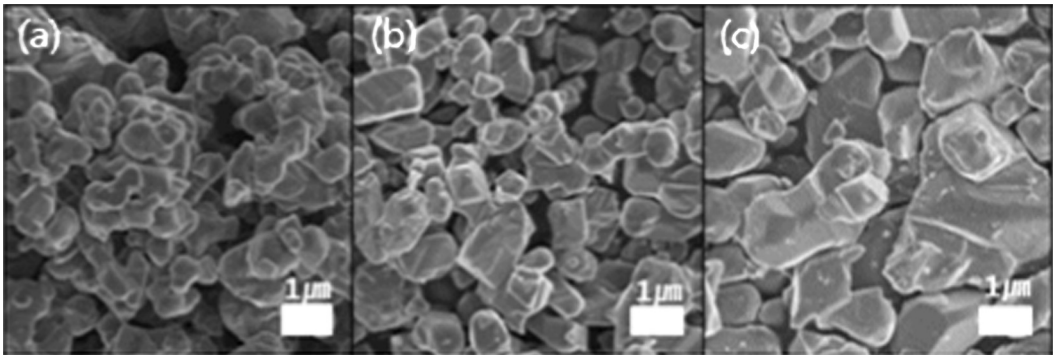

Fig. 4. SEM images of $Li_{(4-x/3)}Al_xTi_{(5-2x/3)}O_{12}$ ($x = 0.1$) samples calcined at (a) 750 °C, (b) 850 °C, and (c) 950 °C.

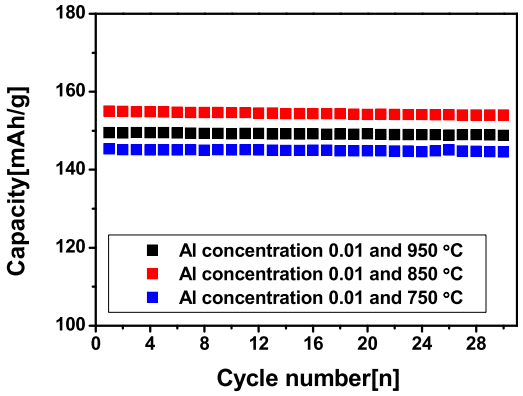

Fig. 5. Cyclic performance of $Li_{(4-x/3)}Al_xTi_{(5-2x/3)}O_{12}$ ($x = 0.01$) samples that were synthesized at three different temperatures (750, 850, 950 °C) at 1C.

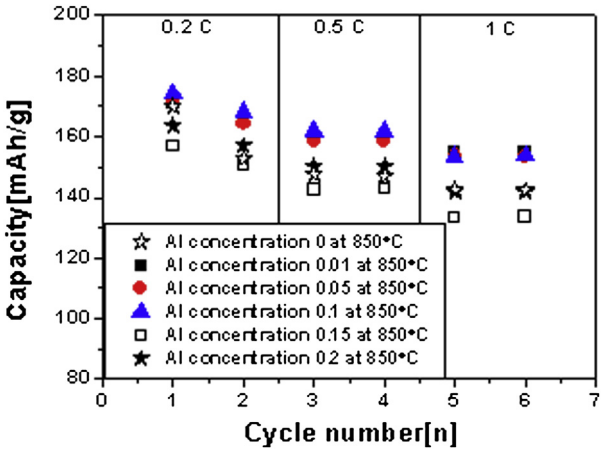

Fig. 6. Variation of discharge capacities of $Li_{4-x/3}Al_xTi_{5-2x/3}O_{12}$ ($x = 0$, 0.01, 0.05, 0.1, 0.15, 0.2) samples at different current densities when the calcination temperature is 850 °C.

Table 1 summarizes the capacity retentions of $Li_{(4-x/3)}Al_xTi_{(5-2x/3)}O_{12}$ ($x = 0.01$, 0.05, 0.1, 0.15, 0.2) after 30 cycles when the synthesized temperature was 850 °C. The Al-doped $Li_4Ti_5O_{12}$ had a higher capacity retention than the undoped $Li_4Ti_5O_{12}$. Almost all the samples had a capacity retention ratio of over 99%. Compared to the capacity retention of 96.14–97.35% after 30 cycles in Al-doped $Li_4Ti_5O_{12}$ that Huang et al. reported [28], this is an improved rate performance. The standard Gibbs energies of Al_2O_3 and Ti_2O_3 were −1576.4 and −1543.9 kJ mol^{-1}, respectively. This indicates a higher stability of the Al–O bond than the Ti–O one in the octahedral coordination polyhedron in the spinel structure. It was suggested that when the titanium was replaced by aluminum in the undoped $Li_4Ti_5O_{12}$ matrix, the stability of the entire spinel structure increased, which could improve the rate capability of the $Li_4Ti_5O_{12}$ materials to some extent [15,27].

Fig. 6 shows the rate performance of $Li_{4-x/3}Al_xTi_{5-2x/3}O_{12}$ ($x = 0$, 0.01, 0.05, 0.1, 0.15, 0.2) samples at different current densities when the calcination temperature is 850 °C, which was the best process temperature. The current density for the first 2 cycles was 0.2C, the second 2 cycles 0.5C, and the third 2 cycles 1C. The $Li_{(4-x/3)}Al_xTi_{(5-2x/3)}O_{12}$ ($x = 0.01$, 0.05, 0.1) samples had a higher capacity than the $Li_{(4-x/3)}Al_xTi_{(5-2x/3)}O_{12}$ ($x = 0$, 0.15, 0.2) at each current density. The first discharge capacities at 0.2, 0.5 and 1C were 174.4, 161.9 and 153.8 mAh g^{-1}, respectively, for $Li_{(4-x/3)}Al_xTi_{(5-2x/3)}O_{12}$ ($x = 0.1$). These capacity values are similar to those of $x = 0.05$ and 0.1. The rate capability of lithium insertion and desertion based material is determined by its lithium-ionic and electronic conductivities. Substitution of Al^{3+} for Li^+ in $Li_4Ti_5O_{12}$ generates a mixing valence of Ti^{3+}/Ti^{4+} as charge compensation and thereby increases the electronic conductivity of $Li_4Ti_5O_{12}$ [5,6,14]. The capacity increase of the doped samples can be explained as follows. During the lithiation process, 3 Li-ions can be accommodated by $Li_4Ti_5O_{12}$, which are transformed to $Li_7Ti_5O_{12}$. In this process, all Li-ions in the 8a-sites and the newly inserted ones move to the octahedral 16c sites. A more stable spinel structure in Al^{3+}-doped $Li_4Ti_5O_{12}$ was formed by a strong Al–O bond. This stable structure may efficiently facilitate the insertion of outside Li-ions into the spinel structure. This is contrary to the Mo-ion substituted $Li_4Ti_5O_{12}$ that showed a decrease of capacity [31].

Fig. 7 shows the discharge profiles of pure $Li_4Ti_5O_{12}$ and $Li_{(4-x/3)}Al_xTi_{(5-2x/3)}O_{12}$ ($x = 0.01$, 0.05, 0.1, 0.15, 0.2) at a current rate of 0.2C between the cut-off voltages of 1.0 and 3.0 V. The samples were synthesized at 850 °C. All the samples had voltage platforms at about 1.5 V. The first discharge capacities were 170.2, 171.0, 171.7, 174.4, 156.8 and 163.8 mAh g^{-1} for $Li_{(4-x/3)}Al_xTi_{(5-2x/3)}O_{12}$ ($x = 0$, 0.01, 0.05, 0.1, 0.15, 0.2), respectively.

As the quantity of Al^{3+} increased to a certain amount ($x = 0$, 0.01, 0.05, 0.1), the capacity of the cell increased at the first discharge. Then the capacity of the cell decreased with more substitution of Al^{3+} into $Li_4Ti_5O_{12}$ ($x = 0.15$, 0.2). The capacity of $Li_4Ti_5O_{12}$ with 0.01, 0.05, 0.1 at% Al was higher than that of undoped lithium titanate. This suggests that the capacity degradation in the high Al^{3+} doping range ($x = 0.15$, 0.2) is induced by a strong impurity effect that compensates for the positive effect of capacity improvement by Al^{3+} doping.

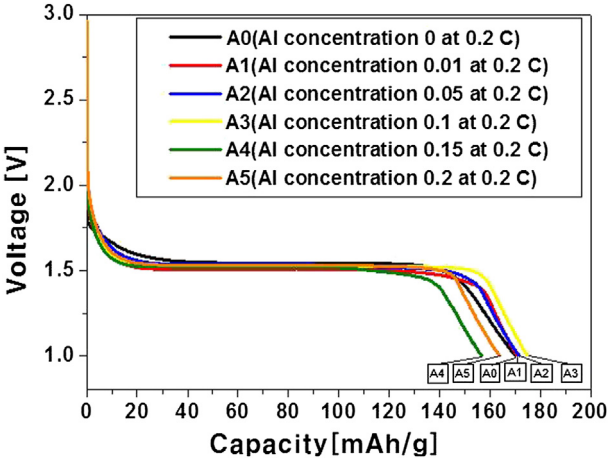

Fig. 7. Discharge curves of pure $Li_4Ti_5O_{12}$ and $Li_{(4-x/3)}Al_xTi_{(5-2x/3)}O_{12}$ ($x = 0$, 0.01, 0.05, 0.1, 0.15, 0.2) at a current rate of 0.2C between the cut-off voltages of 1.0 and 3.0 V.

Table 1
Capacity retention ratios of $Li_{(4-x/3)}Al_xTi_{(5-2x/3)}O_{12}$ ($x = 0$, 0.01, 0.05, 0.1, 0.15, 0.2) samples.

$Li_4Ti_5O_{12}$ ($x = 0$)	$Li_{4-x/3}Al_xTi_{5-2x/3}O_{12}$ ($x = 0.01$)	$Li_{4-x/3}Al_xTi_{5-2x/3}O_{12}$ ($x = 0.05$)	$Li_{4-x/3}Al_xTi_{5-2x/3}O_{12}$ ($x = 0.1$)	$Li_{4-x/3}Al_xTi_{5-2x/3}O_{12}$ ($x = 0.15$)	$Li_{4-x/3}Al_xTi_{5-2x/3}O_{12}$ ($x = 0.2$)
97.4%	99.3%	99.3%	99.3%	99.1%	98.8%

4. Conclusion

The optimum calcination temperature for Al-doped $Li_4Ti_5O_{12}$ was determined to be 850 °C among three temperatures, 750 °C, 850 °C, 950 °C, based on structural and electrochemical characterization. The perfect spinel structure cannot be fully developed at low temperature (750 °C). At high temperature, larger particles are obtained. The larger particle size may result in the reduction of an effective surface area for the lithium-ion conduction path. The doping metal is considered to occupy the 8a tetrahedral sites as well as the 16d octahedral sites. A series of Al^{3+}-doped $Li_{(4-x/3)}Al_xTi_{(5-2x/3)}O_{12}$ (x = 0.01, 0.05, 0.1, 0.15, 0.2) was synthesized at 850 °C. $Li_{(4-x/3)}Al_xTi_{(5-2x/3)}O_{12}$ (x = 0.01, 0.05, 0.1) exhibited better electrochemical performance than $Li_{(4-x/3)}Al_xTi_{(5-2x/3)}O_{12}$ (x = 0, 0.15, 0.2). The 0.1 at.% Al doped $Li_4Ti_5O_{12}$ exhibited capacities of 174.4, 161.9 and 153.8 mAh g^{-1} at 0.2, 0.5 and 1C, respectively, which are similar values to the $Li_{(4-x/3)}Al_xTi_{(5-2x/3)}O_{12}$ (x = 0.01, 0.05). The three samples of $Li_{(4-x/3)}Al_xTi_{(5-2x/3)}O_{12}$ (x = 0.01, 0.05, 0.1) had a capacity retention of over 99.3% after 30 cycles, which was an excellent cycling performance. The good rate performance of $Li_{(4-x/3)}Al_xTi_{(5-2x/3)}O_{12}$ (x = 0.01, 0.05, 0.1) may have originated from the enhanced stability of the spinel structure by stronger Al–O bonding than in the Ti–O bonding. The capacity increase in the doping range of $0.01 \leq x \leq 0.1$ in $Li_{(4-x/3)}Al_xTi_{(5-2x/3)}O_{12}$ was explained by the smooth and efficient insertion of lithium into 16c sites of Al-doped $Li_4Ti_5O_{12}$ in the more stable spinel structure. The poor electrochemical properties of highly Al-doped $Li_{(4-x/3)}Al_xTi_{(5-2x/3)}O_{12}$ (x = 0.15, 0.2) may be due to second impurity phases of TiO_2. Even if a negligible amount of impurity was detected in the XRD patterns of Al-doped $Li_{(4-x/3)}Al_xTi_{(5-2x/3)}O_{12}$ (x = 0.01, 0.05, 0.1), its effect on the electrochemical performance is believed to be insignificant.

Acknowledgement

This work was financially supported by a basic research program (11-EN-03) through the Daegu-Gyeongbuk Institute of Science and Technology (DGIST) funded by the Ministry of Education, Science and Technology (MEST)

References

[1] K.D. Shyamal, A.J. Bhattacharyya, J. Phys. Chem. 113 (2009) 17367–17371.
[2] T. Ohzuku, A. Ueda, N. Yamamoto, J. Electrochem. Soc. 142 (1995) 1431–1435.
[3] T. Ohzuku, A. Ueda, N. Yamamoto, J. Electrochem. Soc. 142 (1995) 1431.
[4] S. Scharner, W. Weppner, P.S. Beurmann, J. Electrochem. Soc. 146 (1999) 857.
[5] P. Martl'n, M.L. Lo'pez, C. Pico, M.L. Veiga, Solid State Sci. 9 (2007) 521–526.
[6] Y.J. Hao, Q.Y. Lai, J.Z. Lu, X.Y. Ji, Ionics 13 (2007) 369–373.
[7] Y.R. Jhan, C.Y. Lin, J.G. Duh, Mater. Lett. 65 (2011) 2502–2505.
[8] B. Zhang, Z. Huang, S. Oh, J. Kim, J. Power Sources 196 (2011) 10692–10697.
[9] B. Tian, H. Xiang, L. Zhang, Z. Li, H. Wang, Electrochim. Acta 55 (2010) 5453–5458.
[10] B. Zhang, H. Du, B. Li, F. Kang, Electrochem. Solid State Lett. 13 (2010) A36–A38.
[11] B.H. Choi, D.J. Lee, M.J. Ji, Y.J. Kwon, S.T. Park, J. Kor. Ceram. Soc. 47 (2010) 638–642.
[12] S. Ji, J. Zhang, W. Wang, Y. Huang, Z. Feng, Z. Zhang, Z. Tang, Mater. Chem. Phys. 123 (2010) 510–515.
[13] Y.L. Qi, Y.D. Huang, D.Z. Jia, S.J. Bao, Z.P. Guo, Electrochim. Acta 54 (2009) 4772–4776.
[14] X. Li, M. Qu, Z. Yu, J. Alloys Compd. 487 (2009) L12–L17.
[15] T.F. Yi, J. Shu, Y.R. Zhu, X.D. Zhu, C.B. Yue, A.N. Zhou, R.S. Zhu, Electrochim. Acta 54 (2009) 7464–7470.
[16] D. Capsoni, M. Bini, V. Massarotti, P. Mustarelli, G. Chiodelli, C. Azzoni, M. Mozzati, L. Linati, S. Ferrari, Chem. Mater. 20 (2008) 4291–4298.
[17] H. Ge, N. Li, D.Y. Li, C.S. Dai, D.L. Wang, Electrochem, Commun. 10 (2008) 1031–1034.
[18] S. Huang, Z. Wen, X. Zhu, Z. Lin, J. Power Sources 165 (2007) 408–412.
[19] C.H. Chen, J.T. Vaughey, A.N. Jansen, D.W. Dees, A.J. Kahaian, T. Goacher, M.M. Thackeray, J. Electrochem. Soc. 148 (2001) A102–A104.
[20] Y.R. Jhan, J.G. Duh, J. Power Sources 198 (2012) 294–297.
[21] H. Xiang, B. Tian, P. Lian, Z. Li, H. Wang, J. Alloy Compd. 509 (2011) 7205–7209.
[22] X. Li, M. Qu, Y. Huai, Z. Yu, Electrochim. Acta 55 (2010) 2978–2982.
[23] G.J. Wang, J. Gao, L.J. Fu, N.H. Zhao, Y.P. Wu, T. Takamura, J. Power Sources 174 (2007) 1109–1112.
[24] J.J. Huang, Z.Y. Jiang, Electrochim. Acta 53 (2008) 7756–7759.
[25] Y.S. Lin, J.G. Duh, J. Power Sources 196 (2011) 10698–10703.
[26] E.M. Sorensen, S.J. Barry, H.K. Jung, J.R. Rodinelli, J.T. Vaughey, K.R. Poeppelmeir, Chem. Mater. 18 (2006) 482–489.
[27] S. Huang, Z. Wen, Z. Gu, Z. Zhu, Electrochim. Acta 50 (2005) 4057–4062.
[28] S. Huang, Z. Wen, X. Zhu, Z. Lin, J. Electrochem. Soc. 152 (2005) A186–A190.
[29] H. Zhao, Y. Li, Z. Zhu, J. Lin, Z. Tian, R. Wang, Electrochim. Acta 53 (2008) 7079–7083.
[30] A.D. Robertson, H. Tukamoto, J.T.S. Irvine, J. Electrochem. Soc. 146 (1999) 3958.
[31] X.L. Zhang, G.R. Hu, Z.D. Peng, J. Inorg. Mat. 26 (2011) 443–448.